# Pulmonary vein reentry—Properties and size matter: Insights from a computational analysis

Elizabeth M. Cherry, PhD,*† Joachim R. Ehrlich, MD,‡ Stanley Nattel, MD,§ Flavio H. Fenton, PhD*‖

*From the *Department of Biomedical Sciences, College of Veterinary Medicine, Cornell University, Ithaca, New York, †Department of Physics and Astronomy, Hofstra University, Hempstead, New York, ‡Division of Cardiology, Section of Electrophysiology, J. W. Goethe-Universität, Frankfurt, Germany, §Research Center, Montreal Heart Institute and Université de Montréal, Montreal, Ontario, Canada, ‖The Heart Institute, Beth Israel Medical Center, New York, New York.*

**BACKGROUND** Pulmonary vein (PV) ablation plays an important role in atrial fibrillation (AF) therapy but suffers from a limited mechanistic understanding of PV arrhythmogenicity. Rapid focal activation has been suggested, but some evidence points to underlying reentry.

**OBJECTIVE** This study was performed to evaluate how the electrophysiological properties of PVs may make them a site for reentry and to analyze specifically the roles of PV dimensions and coupling properties.

**METHODS** A computer model designed to efficiently reproduce electrophysiological behaviors was fit to action potentials from canine left atria (LA) and PVs. To assess structural and functional arrhythmogenic determinants, an idealized PV of varying length and circumference was attached to LA tissue, and 5 seconds of activity after extrastimulation were simulated.

**RESULTS** PV reentrant activity depended critically on vein size and coupling properties. With cumulative removal of transverse and longitudinal connections, sustained (n = 23) or nonsustained (n = 93) reentries could be observed (687 simulations) for veins 1–3 cm long and 1–2 cm in circumference. The prevalence of sustained reentry increased with PV length (8% for 1 cm vs. 22% and 31% for 2 and 3 cm, respectively; $P < .05$ for each). The PV circumference did not affect the incidence of sustained reentry (25%, 17%, and 21% for 1-, 1.5-, and 2-cm circumferences; $P =$ NS), but the number of reentrant events increased from 12/201 simulations for PVs with a 1-cm circumference to 48/232 and 56/254 events for PVs with 1.5- and 2-cm circumferences, respectively ($P < .05$). Sustained reentry cycle lengths were approximately 200–250 ms (16/23), except for the longest PVs.

**CONCLUSION** Reentry occurs readily in PVs with realistic properties in the context of specific connection heterogeneities. Reentry properties and incidence depend on PV anisotropy and dimensions but could certainly contribute significantly to PV arrhythmogenesis.

**KEYWORDS** Catheter ablation; Arrhythmia mechanism; Ion channels; Remodeling; Atrial fibrillation; Therapy; Mathematical models; Ion currents; Reentry

(Heart Rhythm 2007;4:1553–1562) © 2007 Heart Rhythm Society. All rights reserved.

## Introduction

Unraveling the role of pulmonary veins (PVs) in atrial fibrillation (AF) remains an important goal for experimental and clinical research. Since the first note on the importance for AF initiation and maintenance,[1] a large number of studies (at both the basic and clinical science levels) have been devoted to deciphering the mechanisms of PV arrhythmogenicity. Despite this effort, a precise mechanistic understanding has yet to evolve.

In line with initial clinical observations of rapid focal activity within the PVs, one experimental study found triggered arrhythmia due to delayed and early after-depolarizations along with increased pacemaker current in native PVs, which became exaggerated under conditions of tachycardia remodeling.[2] Other work observed triggered activity only under specific conditions such as calcium overload or neurohumoral stimulation.[3,4] Other studies were unable to demonstrate any focal arrhythmias.[5–8] PV cardiomyocytes express a specific profile of ionic currents leading to shorter action potential (AP) duration (APD) in comparison with left atrial (LA) tissue.[6] Impulse propagation within PVs is highly anisotropic owing to fiber arrangement (abrupt direction shifts and circumferential orientations) with reduced connexin (Cx) expression.[5,9] These observations suggested that PVs may have a substrate that is suitable for reentry and point to a possible reentrant mechanism of PV arrhythmo-

This study was supported by National Institutes of Health grants nos. 5F32HL73604 (to EMC) and R01 HL075515 (to FHF), by a Deutsche Forschungsgemeinschaft grant (no. EH 201/2-1, to JRE), and by the Canadian Institutes of Health Research and the Mathematics of Information Technology and Complex Systems Network (SN). The research was facilitated by National Science Foundation grant no. MRI-0320865 and by an allocation of advanced computing resources through the support of the National Science Foundation. **Address reprint requests and correspondence:** Flavio H. Fenton, T7 012C Veterinary Research Tower, Department of Biomedical Sciences, College of Veterinary Medicine, Cornell University, Ithaca, New York, 14853. E-mail address: fhf3@cornell.edu. (Received July 21, 2007; accepted August 15, 2007.)

 © 2007 Heart Rhythm Society. All rights reserved. doi:10.1016/j.hrthm.2007.08.017

genicity. PV reentry is enhanced with neurohumoral stimulation with acetylcholine or isoproterenol.[8,10] Clinical observations of PV reentry have been made in small patient series.[11,12] Based on the AP and coupling properties of PV cardiomyocytes, we hypothesized that PVs may serve as a site for reentry, which may depend critically on PV size and coupling properties. To probe this possibility, we created a mathematical model that accurately reproduces the known AP properties of PV and LA cardiomyocytes and then performed *in silico* analysis to determine whether these properties would allow for preferential PV reentry. To vary coupling over a range of clinically relevant inhomogeneous fiber arrangement conditions, we removed longitudinal or transverse intercellular connections according to a randomization scheme.

## Methods

### Model generation and validation

Using previously reported data,[6] we created a computationally efficient model of canine LA and PV myocyte APs (Figure 1). This formulation differs from more complex ionic models in that instead of reproducing as many individual currents as possible, it is designed to account for the sum of all the currents represented in three main categories: fast inward, slow inward, and slow outward currents. We have previously shown that these currents retain enough structure of the currents involved in cardiac excitation to reproduce AP morphologies accurately under a wide range of physiologically relevant conditions.[13,14] Model parameters can be fitted to replicate properties and dynamics of more complex ionic models as well as of experimental data, such as APD and conduction velocity restitution curves, thresholds for excitation, upstroke velocities, and diastolic intervals.

The differential equations for the model voltage $u$ and gates $v$, $w$, and $s$ are as follows:

$$\frac{du}{dt} = -(I_{fi} + I_{si} + I_{so}),$$

$$\frac{dv}{dt} = \frac{(1 - \mathrm{H}(u - u_c))(1 - v)}{\tau_v^-} - \frac{\mathrm{H}(u - u_c)v}{\tau_v^+},$$

$$\frac{dw}{dt} = \frac{(1 - \mathrm{H}(u - u_c))(1 - w)}{\tau_w^-} - \frac{\mathrm{H}(u - u_c)w}{\tau_w^+}, \text{ and}$$

$$\frac{ds}{dt} = r_s(0.5(1 + \tanh((u - u_{c,si})k)) - s),$$

where

$$\tau_v^- = \tau_{v2}^- \mathrm{H}(u - u_v) + \tau_{v1}^-(1 - \mathrm{H}(u - u_v)),$$

$$\tau_w^- = \tau_{w2}^- \mathrm{H}(u - u_w) + \tau_{w1}^-(1 - \mathrm{H}(u - u_w)),$$

and

$$r_s = r_s^+ \mathrm{H}(u - u_c) + r_s^-(1 - \mathrm{H}(u - u_c)).$$

The transmembrane currents were computed using the following equations:

$$I_{fi} = \frac{-v\,\mathrm{H}(u - u_c)\,(u - u_c)\,(u_m - u)}{\tau_d},$$

$$I_{si} = \frac{-ws}{\tau_{si}}, \text{ and}$$

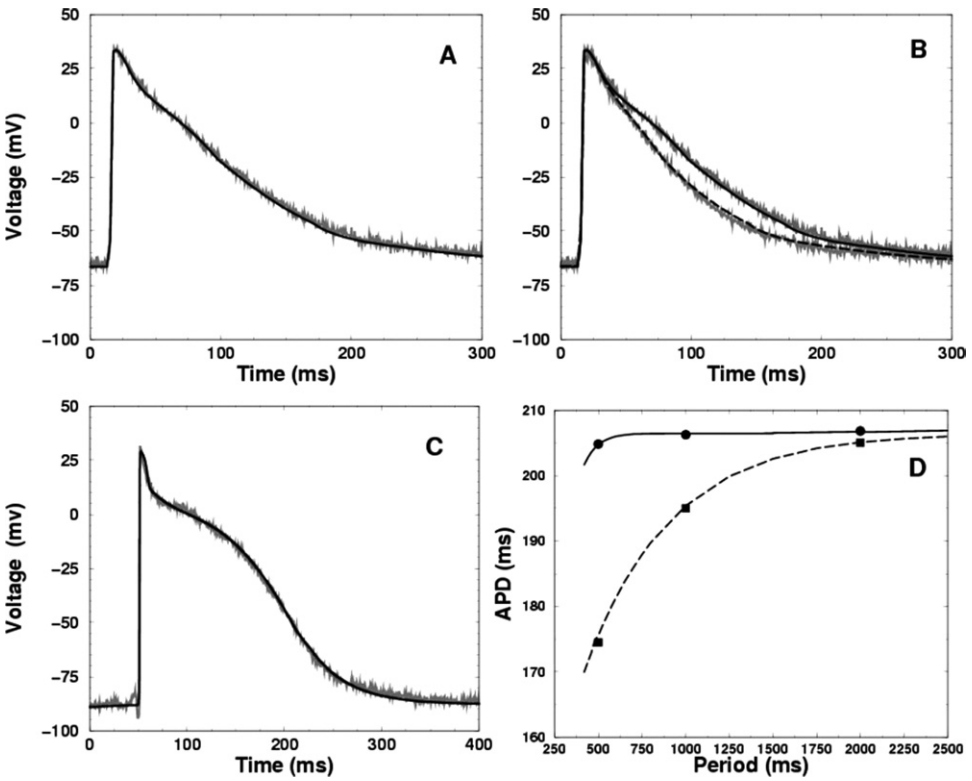


**Figure 1** Generated model APs for LA and PV cardiomyocytes were in good agreement with the experimental data on which they were based. **(A, B)** The PV exhibited stronger rate dependence, and the model captures correct AP morphologies for CLs of both **(A)** 2000 ms (experimental, *gray*; model, *black solid*) and **(B)** 500 ms (experimental, *gray*; model, *black dashed*). **(C)** In contrast, the LA exhibited minimal rate dependence and is shown at a CL of 1000 ms (experimental, *gray*; model, *black solid*). Characteristically, the LA AP had more negative resting membrane potential (−88 vs. −65 mV), larger AP amplitude (118 vs. 99 mV), and less triangular morphology than the PV AP. **(D)** Rate adaptation of $APD_{90}$ for the LA (*solid*) and PV (*dashed*) models compared with experimental results (*filled circles*). In all cases, the model voltage in millivolts is given by rescaling the normalized variable $u$ as $118u$-88.

$$I_{so} = \frac{(u - u_0)(1 - \mathrm{H}(u - u_{so}))}{\tau_{so}} + \mathrm{H}(u - u_{so})\tau_a + 0.5(a_{so} - \tau_a)(1 + \tanh((u - b_{so})/c_{so})),$$

where

$$\tau_{so} = \begin{cases} 1.3\tau_0 & \text{if } u \geq 0.35 \\ (5.25 - 12.8571u)\tau_0 & \text{if } 0.35 > u \geq 0.28 \\ 2.2\tau_0 & \text{if } u < 0.28 \end{cases}$$

for the PV model and $\tau_{so} = \tau_0$ for the LA model. Throughout, the Heaviside function H($x$) had the value of 1 if $x > 0$ and 0 otherwise. The values of all parameters are given in Table 1. Initial conditions were u=0, v=1, w=1 and s=0.

The model successfully reproduces representative AP morphologies for the PV and LA experimental data at different cycle lengths (CLs), as shown in Figures 1A–C. In accordance with experimental findings, rate dependence is more pronounced for the PV model than for the LA model (Figure 1D).

## Creation of three-dimensional PV geometry

To analyze PV-LA interactions, we created a simplified geometry of a single PV attached to a piece of LA (Figure 2). The model is quasi-three-dimensional, with the vein attaching orthogonally to the plane of the LA. The PV itself was topologically a cylinder, as there were no edges, and its length and circumference were varied to investigate the effects of PV dimensions on the induction and maintenance of reentry. The vein representations that were used correspond to the portion of the PVs containing cardiomyocytes, that is, myocardial sleeves. For simplicity, the LA sheet was a square with the same length as the PV (1, 2, or 3 cm). To reproduce periodicity in the atria, periodic boundary conditions were used along one direction of the LA, while zero-flux boundary conditions were used for the other. The LA was paced at a CL of 700 ms to simulate normal sinus rhythm. All simulations lasted 5 seconds. In total, 1067 simulations were performed.

**Table 1** Parameter values for LA and PV models

| Parameter | Value |
|---|---|
| $\tau_v^+$ | 3.33 |
| $\tau_{v1}^-$ | 19.2 |
| $\tau_{v2}^-$ | 10.0 |
| $\tau_w^+$ | 160.0 |
| $\tau_{w1}^-$ | 75.0, 20.0 |
| $\tau_{w2}^-$ | 75.0, 455.0 |
| $\tau_d$ | 0.065, 0.17 |
| $\tau_{si}$ | 31.8364, 47.5304 |
| $\tau_0$ | 39.0, 45.0 |
| $\tau_a$ | 0.009 |
| $u_c$ | 0.23, 0.25 |
| $u_v$ | 0.055 |
| $u_w$ | 0.146 |
| $u_0$ | 0.0, 0.18 |
| $u_m$ | 1.0, 1.05 |
| $u_{c,si}$ | 0.8, 0.85 |
| $u_{so}$ | 0.3, 0.6 |
| $r_s^+$ | 0.02 |
| $r_s^-$ | 1.2 |
| k | 3.0, 5.0 |
| $a_{so}$ | 0.115, 0.025 |
| $b_{so}$ | 0.84, 0.94 |
| $c_{so}$ | 0.02, 0.07 |

Values that differ for LA and PV are given as LA value, PV value.

## Simulation of anisotropic conduction

The LA-PV tissue structure was integrated numerically following the standard cable equation formulation, using the explicit Euler method with a time step of 0.075 ms and a spatial resolution of 0.0125 cm. The diffusion coefficient was set to 0.00025 $cm^2/s$ for the longitudinal cell direction. The transverse diffusion coefficient was set to 10% of the longitudinal diffusion value (in accordance with the normal 10:1 atrial anisotropy ratio) except in the reduced anisotropy case, in which it was set to 20%.

## Randomization procedure

To introduce heterogeneity within the PV, specified fractions of the cell-to-cell connections both longitudinally along the length of the vein and transversely around its circumference were removed, mimicking properties seen histologically. Simulated cells were arranged in a grid. Each of the connections to neighboring cells had a discrete probability of being removed, leaving the cell and its neighbor in that direction disconnected. For convenience, the fractions of connections removed were always multiples of 5. The locations of connection removals were determined at the beginning of a simulation by generating a random number for each longitudinal and transverse connection and setting the corresponding entry in the matrices of the diffusion coefficients to 0 if the random number was lower than the fraction specified for that direction (longitudinal or transverse). The specific locations of disconnections affected propagation patterns within the vein, so results depended to some extent on the specific randomization used. Therefore, simulations were repeated using different randomizations to characterize this effect.

## Data analysis

Reentry was classified as nonsustained (<2 seconds) or sustained (≥2 seconds). Statistical comparison between groups was performed using Fisher's exact test and Student's *t*-test as appropriate.

# Results

Because of the slow and heterogeneous nature of PV propagation, discontinuous conduction could give rise to a reentrant circuit that could activate the LA. Figures 2 and 3 and the accompanying interactive movies (see online Supplement) depict two examples of rapid PV activity caused by circus movement reentry within the PV and driving the LA. In Figure 2, a premature atrial activation induced a PV reentrant wave that repetitively activated the LA. Heterogeneous refractoriness in the vein after the sinus beat blocked

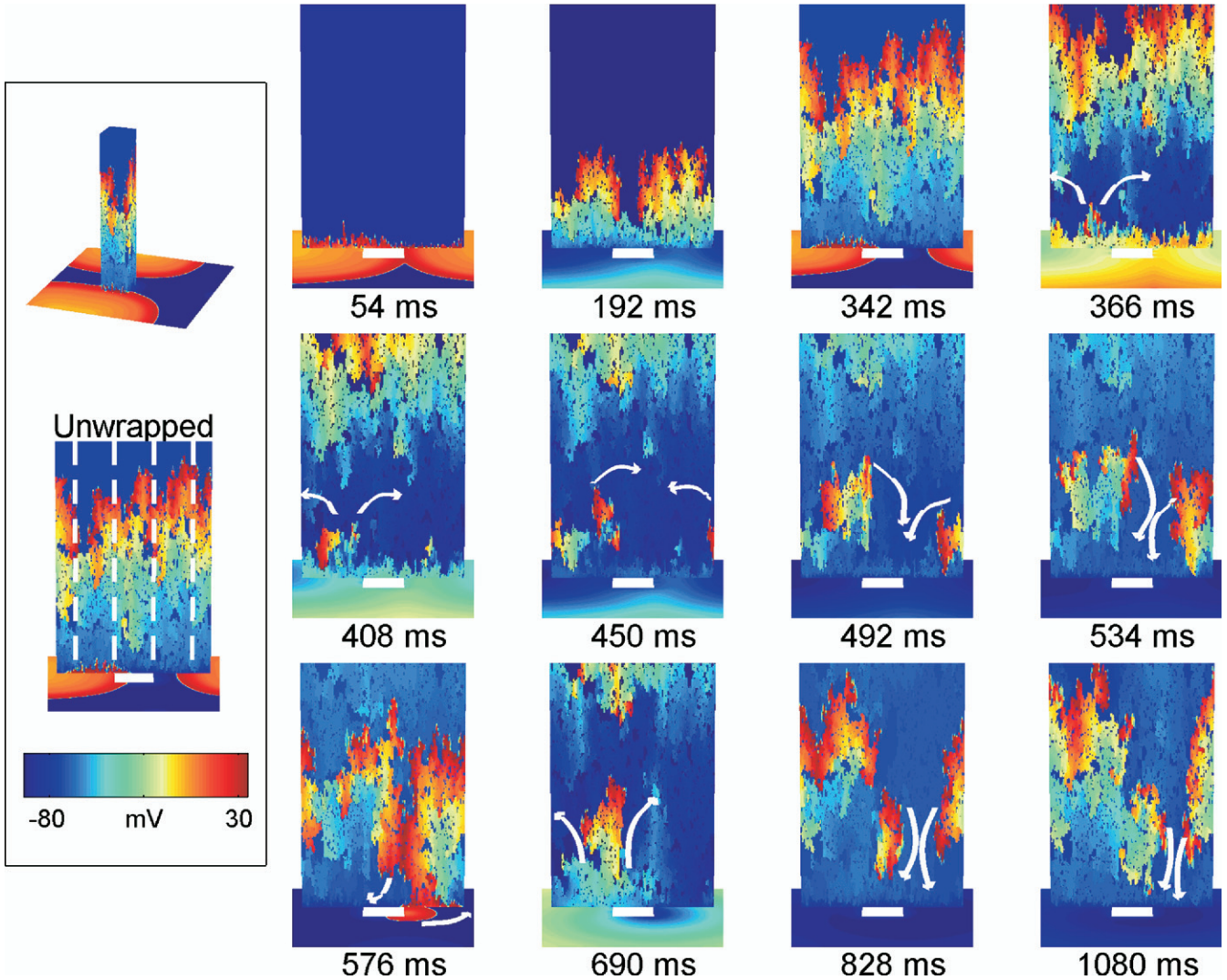


**Figure 2** This figure demonstrates the mechanism of PV activation of the LA due to heterogeneous venous conduction after a premature beat. To allow simultaneous viewing of the entire vein surface, the PV was unwrapped in the figures as indicated on the left. The first sinus beat activated the LA and propagated heterogeneously along the PV, after which the premature beat at time 285 ms reactivated the LA while the vein was primarily refractory from the first beat. Due to the combination of this refractoriness and the heterogeneous conduction within the vein, only a small region of the vein was activated by the premature stimulus. As more of the vein recovered, this small activation in some regions was able to propagate slowly around and then along the vein back toward the LA, following the reentrant circuit indicated by the arrows. After finally reaching the LA-PV junction, it was able to propagate into the LA, which had already recovered from the premature beat. In this sustained reentry, propagation continued within the vein and activated the LA repetitively with a CL of 250 ms. Vein length is 3 cm, and circumference is 2 cm, with 25% longitudinal and 70% transverse disconnections.

the premature beat from propagating within the vein in most locations, but propagation occurred in one area. This small wave initiated a figure-of-8 reentrant circuit along the vein (indicated by the arrows) that repetitively activated the LA at a CL of 250 ms. In Figure 3, a single reentrant beat was initiated without a premature beat. In this case, the heterogeneous conduction of the sinus beat allowed reentry to occur. Two areas largely disconnected from their neighbors closer to the LA were activated by a neighboring area between them, but the large current required to do so caused the area to repolarize more quickly and contributed to block distal to that site. As the wave continued to propagate, it was able to propagate retrogradely toward the LA through the repolarized region and activate the LA.

## Nonsustained and sustained PV reentry

In some cases, reentry was nonsustained (<2 seconds) and activated the LA once or a small number of times. In other cases, reentries were sustained (≥2 seconds) and recurrently activated the LA. Figure 4 illustrates different types of nonsustained and sustained activity that occurred within the PV-activating LA tissue, with premature and simulated sinus beat timings indicated by dotted vertical lines. If a large number of connections remained, activation from the LA propagated along the entire length of the vein. If too few connections remained, activation from the LA was blocked completely and did not propagate along the vein at all. For fractions of connections between these two cases, reentries could develop within

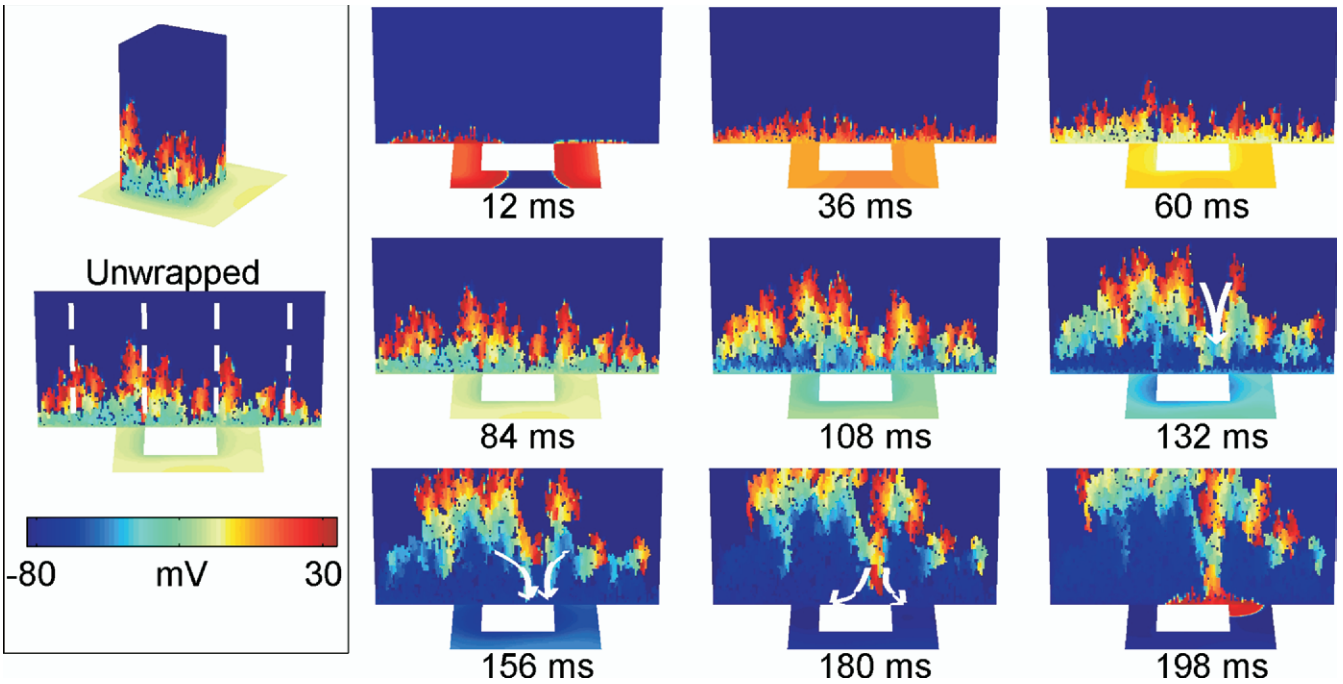


**Figure 3** The mechanism of PV activation of the LA due to heterogeneous venous conduction without the necessity of a premature beat. To allow simultaneous viewing of the entire vein surface, the PV was unwrapped as indicated on the left. The sinus beat propagated heterogeneously along the vein. Because of disconnections, some portions of the vein were not activated as the wave propagated away from the LA but instead were activated as the wave turned and reentered down the length of the vein toward the LA, along the direction of the arrows. The reentrant wave then activated the LA. Vein length is 1 cm, and circumference is 2 cm, with 30% longitudinal and 65% transverse disconnections.

the vein and reactivate the LA sporadically or repetitively (n = 116 of 687 simulations using the nine possible combinations of vein lengths of 1, 2, and 3 cm and circumferences of 1, 1.5, and 2 cm). While the premature beat usually was necessary to induce reentry, this was not always the case, as shown in Figure 3 and in Figure 4A, where reentrant activation occurred before the early beat. However, such reentries (n = 16 of 116) were never sustained and activated the LA at most twice (n = 1 of 16) before self-terminating. With the premature beat present (n = 100 of 116), the LA could be reactivated one (n = 58; Figure 4B) or more (n = 19; Figure 4C) times during a nonsustained reentry (n = 77). For sustained reentries (n = 23), sinus activity in some cases was masked entirely by the driving PV reentry, which prevented all subsequent sinus beats from capturing the LA

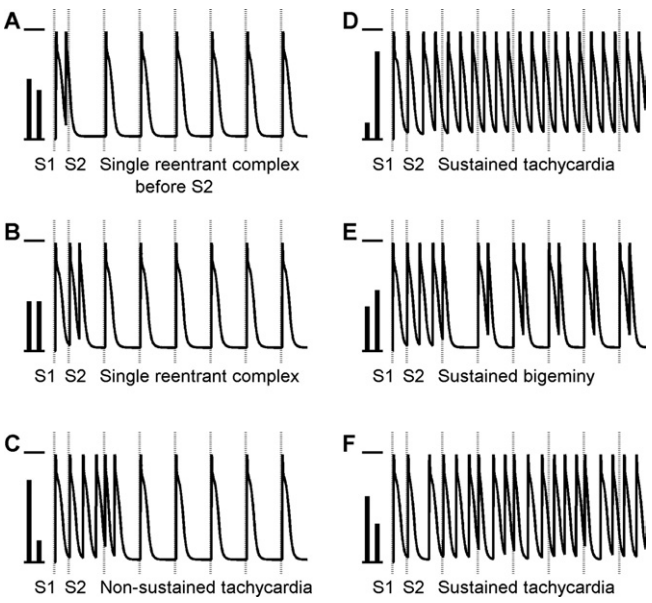


**Figure 4** Types of nonsustained (<2 seconds, **A–C**) and sustained (≥2 seconds, **D–F**) activation of the LA due to heterogeneous conduction leading to reentry within the PV. Both regularly occurring sinus beats and the single premature beat at 285 ms are indicated by *vertical dotted lines*. Five seconds of activity are shown. *Vertical bars* to the left of the trace indicate the percentages of transverse and longitudinal disconnections; *lower and upper horizontal bars* represent 0 and 100% disconnection, respectively. **(A)** In 17% of all nonsustained activity shown in Figure 6 (16 of 93 cases), reentry occurred within the PV and activated the LA before the premature stimulus, which was blocked. Conversely, reentry occurred after the premature stimulus in 77 of 93 cases. **(B)** In 78% of all nonsustained activity shown in Figure 6 (73 of 93 cases), a premature stimulus initiated reentry that produced a single activation in the LA. **(C)** In 22% of all nonsustained activity shown in Figure 6 (20 of 93 cases), multiple activations in the LA were elicited. **(D)** The recurrent activation of the LA was completely independent of subsequent sinus beats for 17% of all sustained activity shown in Figure 6. **(E, F)** For the remaining sustained activity shown in Figure 6, the recurrent LA activation interacted regularly with simulated sinus beats (**E,** 4%) or intermittently (**F,** 78%). Vein length was 3 cm in panel **A,** 1 cm in panel **E,** and 2 cm in all other panels. Vein circumference was 1 cm in panel **C** and 1.5 cm in all other panels. For panels **A–F,** respectively, longitudinal disconnection percentages were 45%, 45%, 20%, 80%, 55%, and 35%; and transverse disconnection percentages were 55%, 45%, 75%, 15%, 40%, and 60%.

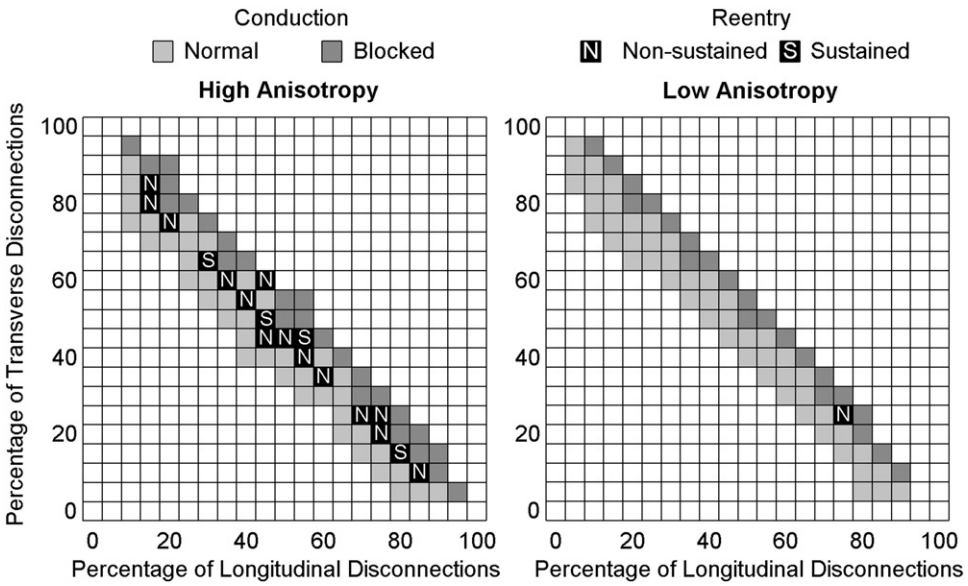


**Figure 5** Behavior resulting from various combinations of longitudinal and transverse heterogeneity for a fixed vein size (2 cm in length, 1.5 cm in circumference) but different anisotropy ratios. The axes show the percentages of longitudinal and transverse cell-to-cell coupling randomly disconnected within the entire PV. *Dark gray* and *light gray* indicate completely blocked and completely normal conduction within the vein, respectively, while *black* indicates nonsustained (N) and sustained (S) reentrant venous activity that propagates to the LA. Untested combinations are shown in *white*. Low anisotropy was obtained with the transverse diffusion coefficient set to 20% of the longitudinal diffusion value instead of 10%. Under these conditions, reentry became more difficult to induce (one of 72 attempts vs. 18 of 84 attempts with high anisotropy). Nonsustained reentry occurred for only one selection of longitudinal and transverse heterogeneity (vs. n = 14 for high anisotropy), while sustained reentry did not occur (vs. n = 4 for high anisotropy).

(n = 4 of 23; Figure 4D). In other cases, the sinus beats interacted with the PV reentry. In rare cases, interactions with sinus beats were necessary to sustain the reentry (n = 1 of 23), which manifest as bigeminy (Figure 4E). Often, sinus activity complicated the LA activation sequence by propagation from PV reentries and by some sinus beats (n = 18 of 23; Figure 4F).

## Role of anisotropic conduction

To assess the coupling conditions associated with sustained reentry, we plotted activity type as a function of longitudinal and transverse disconnection percentages for a given vein length and circumference. Figure 5 indicates activity for combinations of longitudinal and transverse disconnections for a vein of length 2 cm and circumference 1.5 cm with normal (high) and reduced (low) anisotropy. A total of 84 and 72 combinations were tested for this vein size for high and low anisotropy (Figure 5), respectively. When high anisotropy was used, the longitudinal and transverse disconnection percentages that gave rise to nonsustained or sustained reentry occurred along a diagonally oriented band where the sum of the longitudinal and transverse disconnection percentages was between 90 and 105, with four sustained and 14 nonsustained events. Thus, for highly anisotropic tissue, it is primarily the total percentage of connections that matters for reentry induction, rather than the percentage of longitudinal or transverse disconnections alone. Among nonsustained events, eight activated the LA only a single time before terminating (including one that occurred before the premature stimulus), five activated the LA twice, and one activated the LA three times. The effect of low anisotropy was also tested for the same size vein (Figure 5B). Under these conditions, reentry was much more difficult to induce: only one nonsustained reentrant event occurred.

## Influence of PV geometry

Similar plots for different PV lengths (1, 2, and 3 cm) and different circumferences (1, 1.5, and 2 cm) using normal (high) anisotropy are shown in Figure 6. Reentry again occurred along the diagonally oriented band with the sum of the longitudinal and transverse disconnection percentages totaling between 85 and 105. When the absolute numbers of longitudinal and transverse disconnection combinations resulting in reentry and the relative frequency of nonsustained versus sustained reentry were grouped according to vein length or vein circumference, several trends appeared (Figure 7). The absolute number of reentrant events did not vary much with PV length, but the percentage of reentries that were sustained increased with length (Figure 7A), from 8% for a length of 1 cm to 22% and 31% for lengths of 2 and 3 cm, respectively ($P < .05$ each). When the circumference was increased, the percentage of reentries that were sustained remained roughly constant (25%, 17%, and 21%, $P$ = NS), but the absolute number of reentrant events increased from 12 events for a circumference of 1 cm to 48 and 56 events for circumferences of 1.5 and 2 cm, respectively ($P < .05$; Figure 7B). The CLs of sustained reentries did not vary much with either vein length (230.7 ± 6.4, 230.6 ± 13.3, and 287 ± 79.8 ms for lengths of 1, 2, and 3

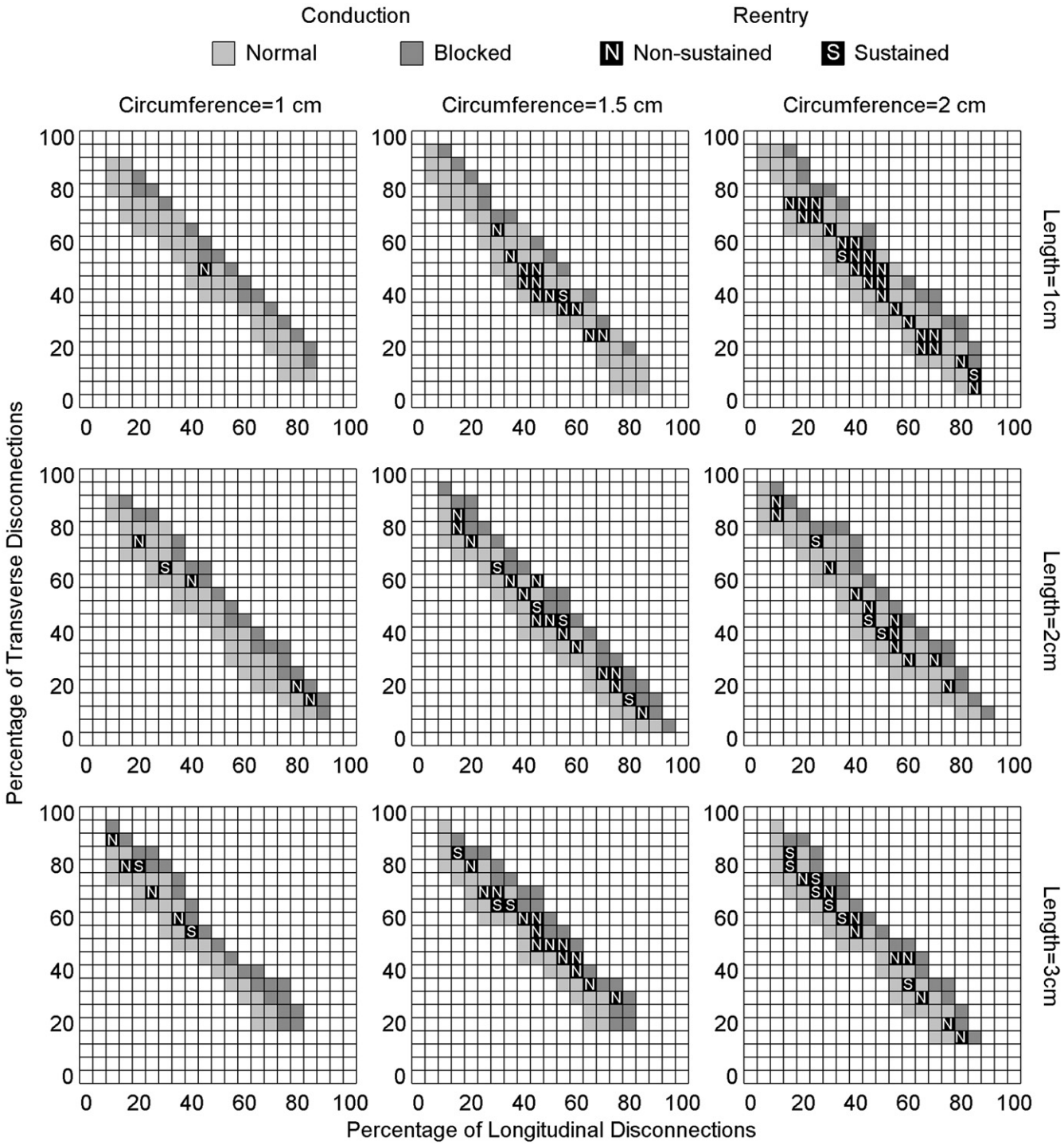


**Figure 6** Behavior resulting from longitudinal and transverse heterogeneity for a range of PV lengths and circumferences. Vein lengths were 1, 2, and 3 cm, while vein circumferences were 1, 1.5, and 2 cm. Results from a total of 687 simulations are shown. *Axes and color scheme* are identical to those in Figure 5; for a detailed description of methods for varying connections/conduction properties, see Figure 5 legend.

cm; $P$ = NS) or vein circumference (261.3 ± 63.3, 251 ± 44.8, and 266.0 ± 77.8 ms for circumferences of 1, 1.5, and 2 cm; $P$ = NS) and fell primarily between 200 and 250 ms (n = 16 of 23). However, the longest vein length of 3 cm also was capable of supporting slower reentries with CLs between 250 and 333 ms (n = 7 of 23; Figure 7C).

## Influence of randomization scheme

Because the propagation pattern depended on the specific locations of disconnections, the series of random numbers generated to specify disconnection locations affected the values of disconnection percentages that resulted in reentry. Figure 8 presents results obtained using four additional

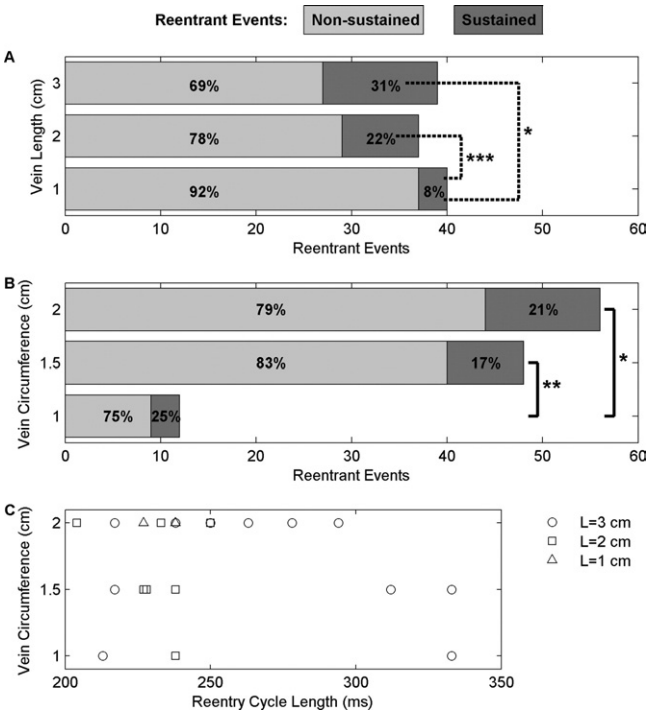


**Figure 7** **(A, B)** Reentrant activity for all nonsustained and sustained reentries shown in Figure 5 as a function of **(A)** vein length and **(B)** vein circumference. The number of reentrant events is plotted, and the percentages of reentries that were nonsustained (*light gray*) and sustained (*dark gray*) are indicated. *$P$ <.05; **$P$ <.01; ***$P$ <.005 compared with the smallest vein length and circumference as indicated. **(C)** Average reentry CL for all non-sinus-dependent sustained reentries shown in Figure 6 as a function of vein circumference and length. The single sinus-dependent reentry was excluded here because its dominant reentry CL matched the sinus CL.

randomization sets for a vein length of 2 cm and circumference of 1.5 cm. When compared with each other and with the high-anisotropy case in Figure 5, which depicts the same size vein using a fifth randomization scheme, the average number of reentrant events was 15.6 ± 4.0, and the average percentage of sustained events was 20.9% ± 12.0%. The number of cases in which reentry developed without the need for the premature beat also varied with the randomization scheme between 0 and 4, with an average of 1.4 ± 2.8 and representing 8.5% ± 1.0% of the reentries. Differences in the specific disconnection values leading to reentry also occurred. However, the average CLs of non-sinus-dependent reentries for the four randomization schemes that produced sustained reentry remained constant (230, 224, 232, and 241 ms; $P$ = NS), and overall trends for the relationship between uncoupling and reentrant activity were qualitatively the same.

## Discussion

AF is a highly prevalent arrhythmia with substantial impact on morbidity, mortality, and health care costs. PV-focused interventional therapy is having a significant impact on AF burden. In the present study, we examined the role of PV properties and geometry in the generation of reentrant PV activation using a computer model.

### PV reentry as a potential mechanism for AF induction and sustenance

Previous clinical observations have highlighted the importance of focal PV activity in initiating AF. The small size of PVs would seem to make PV reentrant activity unlikely; however, previous work indicated a possibility of inducing sustained reentrant tachycardia (with CLs between 114 and 280 ms) within 2.6% of isolated PVs after ablation,[11] and Belhassen et al[15] reported a single case of AF initiated by local reentry within the right superior PV. Most observations of PV reentry in the present study showed tachycardia CLs between 200 and 250 ms, compatible with those observed clinically. Another study in 56 patients showed that PV tachycardia with a CL shorter than that of the LA was present in >80% of superior PVs before ablation and that the inducibility of sustained AF decreased after PV isolation. The investigators accordingly concluded that PV tachycardia may contribute to AF maintenance.[16] Kumagai and coworkers[12] used a 64-pole basket catheter to map human PVs during electrophysiologic study. Focal discharges from the distal PV often initiated reentry at the LA-PV border. Anisotropy in impulse conduction within the vein was important for reentry, in line with the importance of anisotropy in our study. Such behavior of PVs is supported by experimental work demonstrating regional heterogeneity in Cx distribution. Cx40 was predominantly located at the lateral sides of atrial myocytes, and a reduced amount was found in PV tissue, compatible with locally increased anisotropy.[17,9]

Experimental studies of basic PV electrophysiology have identified electrical and structural characteristics distinct from the LA. A detailed characterization of PV features found less negative resting membrane potential owing to reduced $I_{K1}$. Combined with increased delayed rectifier potassium currents and decreased inward calcium currents (consequently shorter AP duration), this suggested a potential substrate for reentry in PVs.[6] PV cardiomyocytes exhibited increased constitutively active Kir3-current leading to enhanced PV repolarization with relevance for tachyarrhythmias. These findings are in line with PVs being a preferred site for reentry.[18,19] Optical mapping demonstrated both focal activity and reentry in PVs.[10] Sustained PV reentry was only inducible after adrenergic stimulation, hinting at the importance of neurohumoral factors. Recent work by Po and coworkers[8] using a combined approach of optical mapping and microelectrode recording confirmed that PVs may provide a favorable substrate for reentry formation. Sustained PV tachycardias required the presence of acetylcholine and were very rapid (mean CL 93 ± 15 ms) and were accompanied by classical electrophysiological criteria for reentry, which was confirmed by optical mapping.

In contrast, other studies observed only nonreentrant focal PV activity after remodeling induced by rapid atrial pacing.[20] Similarly, Honjo et al[3] found ectopic PV activity in remodeled states with interventions leading to intracellular calcium overload like ryanodine or beta-adrenergic stimulation.

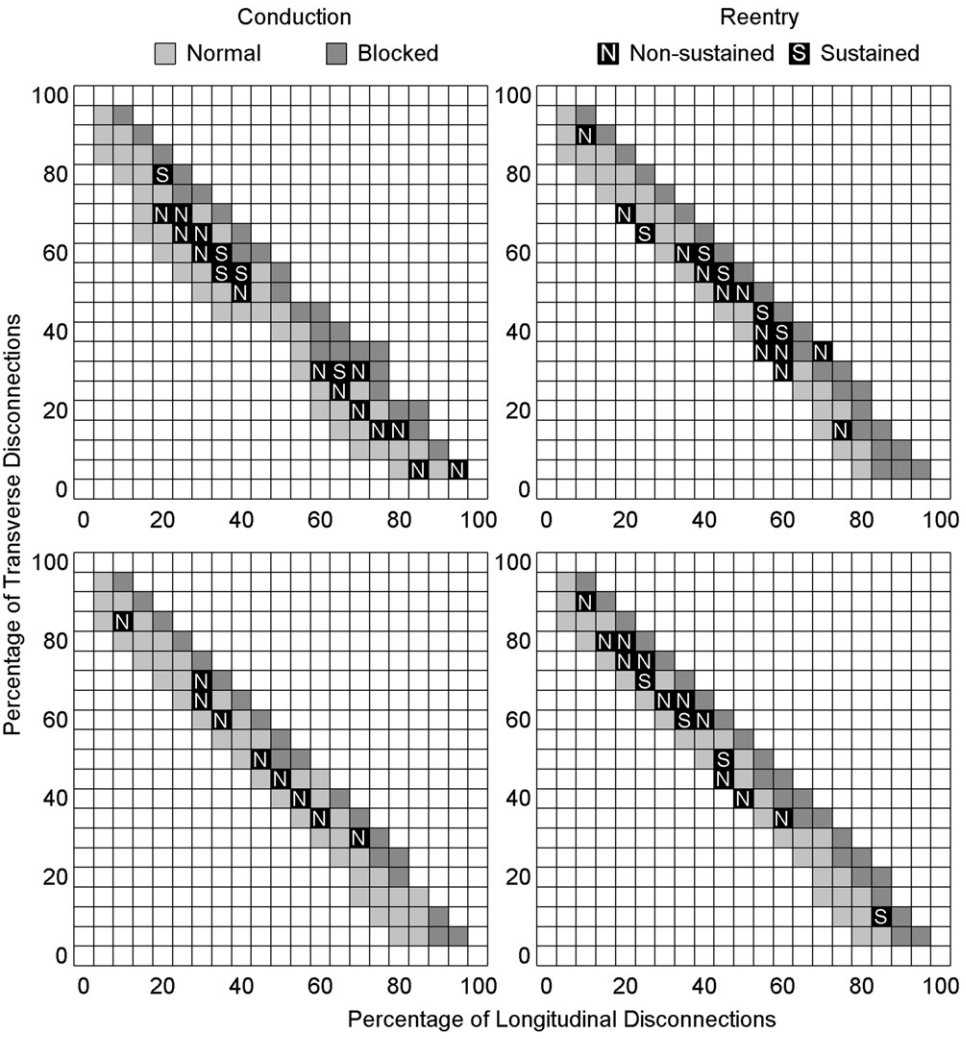


**Figure 8** Behavior resulting from longitudinal and transverse heterogeneity for a fixed vein length (2 cm) and circumference (1.5 cm) but different randomizations of conduction heterogeneity. Results from a total of 308 simulations are shown. *Axes and color scheme* are identical to those in Figure 5; for a detailed description of methods for varying connections/conduction properties, see Figure 5 legend.

## Role of PV size for AF initiation and reentry generation

Our results suggest that PV circumference and length may be important determinants of PV reentry. Our three-dimensional PV was modeled with canine PV sizes rather than with human sizes since the model was based on canine data. A broad range of human PV sizes has been reported, and the circumferences we tested are toward the smaller end.[21,22] Verheule et al[9] reported canine PV myocardial sleeve lengths of 0.4–2.0 cm, similar to the lengths used here. In clinical studies, arrhythmogenic PVs have larger diameters than nonarrhythmogenic PVs,[23] and there is evidence that conditions associated with paroxysmal AF (e.g., arterial hypertension) increase PV diameter, potentially creating conditions for persistent reentry.[24] Similarly, increased atrial pressure leads to faster activation and organization of waves emanating from the PV regions in a sheep model.[25]

## Potential limitations

The randomization has an influence on which specific combinations of connection removals lead to reentry. The sheer number of simulations required prevented us from testing randomization for more than one vein length/circumference combination. The results presented in this manuscript already combine the outcomes of more than 1000 individual simulations. Although the specific numbers of reentrant events and the specific longitudinal and transverse disconnection percentages producing reentry were not identical with different randomizations, we observed the same mechanism giving rise to reentry independent of the randomization used.

This study was performed entirely *in silico* and did not include *in vivo* confirmation, for example, by optical mapping. It would be very interesting to induce PV reentry in intact cardiac preparations, perform optical mapping, and relate the tissue coupling/reentry relationship to model predictions. However, such experiments are beyond our present technical expertise. The complex PV anatomy poses significant obstacles to detailed optical mapping, and it is not presently possible to map electrical coupling of an *in situ* tissue at the microscopic level that would be necessary. Because of these practical limitations, our study was designed to determine whether reported PV AP and coupling properties are sufficient to permit PV reentry and, if so, to define the properties of

such reentry in terms of CL, sustainability, and dependence on PV anatomy and coupling. We were able to show that the known features of the PVs allow reentry to be initiated and maintained within them and that there are specific determinants in terms of PV dimensions and coupling. Some of the predictions of our model are amenable to assessment with present technologies in clinical electrophysiology laboratories, and we hope that experimental methods will advance sufficiently to permit detailed testing within *in situ* systems.

## Conclusion

The present study suggests that PV reentry in PVs can occur with realistic PV properties. PV reentry is dependent on heterogeneous and anisotropic conduction and occurs more frequently in wider veins, while it is more often sustained in longer veins. This work helps to improve our understanding of the potential mechanisms and determinants of PV arrhythmogenic activity.

## Supplementary data

Please see online version of this article to view accompanying videos.

## References


1. Haissaguerre M, Jais P, Shah DC, Takahashi A, Hocini M, Quiniou G, Garrigue S, Le Mouroux A, Le Metayer P, Clementy J. Spontaneous initiation of atrial fibrillation by ectopic beats originating from the pulmonary veins. N Engl J Med 1998;339:659–666.
2. Chen YJ, Chen SA, Chen YC, Yeh HI, Chan P, Chang MS, Lin CI. Effects of rapid atrial pacing on the arrhythmogenic activity of single cardiomyocytes from pulmonary veins: implication in initiation of atrial fibrillation. Circulation 2001; 104:2849–2854.
3. Honjo H, Boyett MR, Niwa R, Inada S, Yamamoto M, Mitsui K, Horiuchi T, Shibata N, Kamiya K, Kodama I. Pacing-induced spontaneous activity in myocardial sleeves of pulmonary veins after treatment with ryanodine. Circulation 2003;107:1937–1943.
4. Patterson E, Po SS, Scherlag BJ, Lazzara R. Triggered firing in pulmonary veins initiated by in vitro autonomic nerve stimulation. Heart Rhythm 2005;2:624–631.
5. Hocini M, Ho SY, Kawara T, Linnenbank AC, Potse M, Shah D, Jais P, Janse MJ, Haissaguerre M, de Bakker JMT. Electrical conduction in canine pulmonary veins. Electrophysiological and anatomic correlation. Circulation 2002;105: 2442–2448.
6. Ehrlich JR, Cha TJ, Zhang L, Chartier D, Melnyk P, Hohnloser SH, Nattel S. Cellular electrophysiology of canine pulmonary vein cardiomyocytes: action potential and ionic current properties. J Physiol 2003;551:801–813.
7. Wang TM, Chiang CE, Sheu JR, Tsou CH, Chang HM, Luk HN. Homogeneous distribution of fast response action potentials in canine pulmonary vein sleeves: a contradictory report. Int J Cardiol 2003;89:187–195.
8. Po SS, Li Y, Tang D, Liu H, Geng N, Jackman WM, Scherlag B, Lazzara R, Patterson E. Rapid and stable re-entry within the pulmonary vein as a mechanism initiating paroxysmal atrial fibrillation. J Am Coll Cardiol 2005;45: 1871–1877.
9. Verheule S, Wilson EE, Arora R, Engle SK, Scott LR, Olgin JE. Tissue structure and connexin expression of canine pulmonary veins. Cardiovasc Res 2002;55: 727–738.
10. Arora R, Verheule S, Scott L, Navarrete A, Katari V, Wilson E, Vaz D, Olgin JE. Arrhythmogenic substrate of the pulmonary veins assessed by high-resolution optical mapping. Circulation 2003;107:1816–1821.
11. Takahashi Y, Iesaka Y, Takahashi A, Goya M, Kobayashi K, Fujiwara H, Hiraoka M. Reentrant tachycardia in pulmonary veins of patients with paroxysmal atrial fibrillation. J Cardiovasc Electrophysiol 2003;14:927–932.
12. Kumagai K, Ogawa M, Noguchi H, Yasuda T, Nakashima H, Saku K. Electrophysiologic properties of pulmonary veins assessed using a multielectrode basket catheter. J Am Coll Cardiol 2004;43:2281–2289.
13. Fenton F, Karma A. Vortex dynamics in three-dimensional continuous myocardium with fiber rotation: filament instability and fibrillation. Chaos 1998;8:20–47.
14. Fenton FH, Cherry EM, Hastings HM, Evans SJ. Multiple mechanisms of spiral wave breakup in a model of cardiac electrical activity. Chaos 2002;12:852–892.
15. Belhassen B, Glick A, Viskin S. Reentry in a pulmonary vein as a possible mechanism of focal atrial fibrillation. J Cardiovasc Electrophysiol 2004;15:824–828.
16. Oral H, Ozaydin M, Tada H, Chugh A, Scharf C, Hassan S, Lai S, Greenstein R, Pelosi F Jr, Knight BP, Strickberger SA, Morady F. Mechanistic significance of intermittent pulmonary vein tachycardia in patients with atrial fibrillation. J Cardiovasc Electrophysiol 2002;13:645–650.
17. Polontchouk L, Haefliger JA, Ebelt B, Schaefer T, Stuhlmann D, Mehlhorn U, Kuhn-Regnier F, De Vivie ER, Dhein S. Effects of chronic atrial fibrillation on gap junction distribution in human and rat atria. J Am Coll Cardiol 2001;38: 883–891.
18. Ehrlich JR, Cha TJ, Zhang L, Chartier D, Villeneuve L, Hebert TE, Nattel S. Characterization of a hyperpolarization-activated time-dependent potassium current in canine cardiomyocytes from pulmonary vein myocardial sleeves and left atrium. J Physiol 2004;557:583–597.
19. Cha TJ, Ehrlich JR, Chartier D, Qi XY, Xiao L, Nattel S. Kir3-based inward rectifier potassium current: potential role in atrial tachycardia remodeling effects on atrial repolarization and arrhythmias. Circulation 2006;113:1730–1737.
20. Zhou S, Chang CM, Wu TJ, Miyauchi Y, Okuyama Y, Park AM, Hamabe A, Omichi C, Hayashi H, Brodsky LA, Mandel WJ, Ting CT, Fishbein MC, Karagueuzian HS, Chen PS. Nonreentrant focal activations in pulmonary veins in canine model of sustained atrial fibrillation. Am J Physiol Heart Circ Physiol 2002;283:H1244–H1252.
21. Kok LC, Everett TH, Akar JG, Haines DE. Effect of heating on pulmonary veins: how to avoid pulmonary vein stenosis. J Cardiovasc Electrophysiol 2003;14:250–254.
22. Feld GK, Yao B, Reu G, Kudaravalli R. Acute and chronic effects of cryoablation of the pulmonary veins in the dog as a potential treatment for focal atrial fibrillation. J Interv Card Electrophysiol 2003;8:135–140.
23. Yamane T, Shah DC, Jais P, Hocini M, Peng JT, Deisenhofer I, Clementy J, Haissaguerre M. Dilatation as a marker of pulmonary veins initiating atrial fibrillation. J Interv Card Electrophysiol 2002;6:245–249.
24. Herweg B, Sichrovsky T, Polosajian L, Rozenshtein A, Steinberg JS. Hypertension and hypertensive heart disease are associated with increased ostial pulmonary vein diameter. J Cardiovasc Electrophysiol 2005;16:2–5.
25. Kalifa J, Jalife J, Zaitsev AV, Bagwe S, Warren M, Moreno J, Berenfeld O, Nattel S. Intra-atrial pressure increases rate and organization of waves emanating from the superior pulmonary veins during atrial fibrillation. Circulation 2003;108:668–671.